PERGAMON

International Journal of Heat and Mass Transfer 43 (2000) 1679–1698

International Journal of HEAT and MASS TRANSFER

www.elsevier.com/locate/ijhmt

General solutions for stationary/moving plane heat source problems in manufacturing and tribology

Z.B. Hou, R. Komanduri*

Mechanical and Aerospace Engineering, Oklahoma State University, Stillwater, OK 74078, USA

Received 20 April 1999; received in revised form 23 August 1999

Abstract

General solutions (both *transient* and *steady state*) for the temperature rise at any point due to stationary/moving plane heat sources of different shapes (*elliptical*, *circular*, *rectangular*, and *square*) and heat intensity distributions (*uniform*, *parabolic*, and *normal*) are presented using the Jaeger's classical *heat source method* (J.C. Jaeger, Moving sources of heat and the temperature at sliding contacts, Proc. Royal Society of NSW 76 (1942) 203–224). Starting from an instantaneous point heat source solution, an *elliptical moving heat source* with different heat intensity distributions, namely, uniform, parabolic and normal, was used as the *basic plane heat source* and its solution for the temperature rise at any point was derived. This analysis was then extended to other plane heat sources, such as circular, rectangular, and square heat sources to cover a range of manufacturing processes and tribological problems experienced in engineering practice. In addition, the analysis presented here is valid for *both transient and steady state conditions* while most analyses to date are strictly for quasi-steady state conditions. The solutions for the stationary heat sources are obtained from the moving heat source solution by simply equating the velocity of sliding to zero. Further, the analysis can be used to determine the *temperature distribution not only at the surface* but also *with respective to the depth* which again is a very important consideration in most manufacturing and tribological applications since it effects the subsurface deformation, metallurgical changes, hardness variation, and residual stresses. It can also be used to determine the *maximum and average temperatures* within the area of the heat source. Thus, the analysis presented here is believed to be comprehensive. © 2000 Elsevier Science Ltd. All rights reserved.

1. Introduction

Plane heat source problems (both stationary and moving) are frequently encountered in numerous manufacturing processes, such as metal cutting (shear plane heat source and frictional heat source at the chip-tool interface), grinding, and polishing; spot welding (conventional and nonconventional) and cutting (gas-arc, plasma-arc, laser); surface heat treatment using laser irradiation; and EDM machining of openings of various shapes (relative to the EDM tools) as well as in many tribological applications, such as meshing of gears, cams, bearings, asperities in sliding contact. The relevant thermal analysis for these applications begins with the solution of a plane heat source of appropriate shape and heat intensity distribution. Temperature distribution and the rate of cooling at and near the surface can affect the metallurgical microstructure, thermal shrinkage, thermal cracking, hardness distribution, residual stresses, heat affected zone (HAZ), and chemical modifications of the material.

* Corresponding author. Tel.: +1-405-744-5900; fax: +1-405-744-7873.

E-mail address: ranga@ceat.okstate.edu (R. Komanduri).

0017-9310/00/$ - see front matter © 2000 Elsevier Science Ltd. All rights reserved.
PII: S0017-9310(99)00271-9

Nomenclature

a_o, b_o	semi-major and semi-minor axes of an elliptical heat source or half the side of a rectangular heat source. When $a_o = b_o$ radius of a circular heat source or half the side of a square heat source
a	thermal diffusivity of the medium (cm^2/s)
A_{pl}, A_{ell}, A_c, A_{rec}, A_{sq}	area of a plane, elliptical ($=\pi a_o b_o$), circular ($=\pi r_o^2$), rectangular ($=4a_o b_o$), and square ($=4a_o^2$) heat sources, respectively (cm^2)
c	specific heat (J/g·°C)
l, L	semi-width and width of the heat source along the direction of motion
l_{y_i}	half length of a differential stripe with a distance from the center of the elliptical source y_i (cm)
m, n	x_i/a_o (or X_i/a_o) and y_i/b_o, respectively
Q_{pt}	amount of heat liberated by the instantaneous point heat source (J)
q_{pt}	heat liberation rate of a stationary point heat source (J/s)
q_{pl}, q_{ell}, q_c, q_{rec}, q_{sq}	heat liberation rate of stationary/moving plane, elliptic, circular, rectangular, and square heat sources, respectively (J/s)
q_o	heat liberation intensity of a plane heat source (J/cm^2·s)
R	distance between the stationary/moving point heat source and the point where the temperature rise at time t is concerned (cm)
R_i	distance between the differential segmental heat source and the point where the temperature rise at time t is concerned (cm)
τ	the time after the initiation of an instantaneous heat source (s)
t	time of observation or the time after the initiation of a continuous heat source (s)
x_i, y_i	coordinates of a differential segmental element from the plane heat source of various shapes
x, y, z	coordinates of the point M where the temperature rise is concerned
X_i, y_i	coordinates of a differential segmental element from the plane heat source of various shapes in a moving coordinate system
X, y, z	coordinates of the point M where the temperature rise is concerned, in a moving coordinate system
λ	thermal conductivity of the medium (J/cm·s·°C)
θ	temperature rise at any point at any time t (°C)
θ_M	temperature rise at any point M at any time t (°C)
ρ	density of the medium (g/cm^3)
$K_m(u_i)$	$=\int_0^{v^2 t/4a} \frac{d\omega}{\omega^{3/2}} e^{-\omega - u_i^2/4\omega}$ where $u_i = \frac{R_i v}{2a}$
erf $c(p)$	complementary error function ($1 - \mathrm{erf}(p) = 1 - \frac{2}{\sqrt{\pi}} \int_p^\infty e^{-u^2}\, du$)

These effects are collectively termed as *surface integrity* problems. Consequently, thermal aspects of manufacturing are critical in the optimization of the process parameters and quality of the products produced as well as their performance and reliability in service.

It may be noted that solutions of plane heat source problems (both stationary and moving) of various shapes and heat intensity distributions using the partial differential equations (PDE) method directly may not be simple and straightforward for they encounter boundaries where the temperatures are unknown and only the heat fluxes are known (either a constant value or a known function). Thus, to define and express it mathematically may not be simple. Even if so, it is still not certain whether it would be possible to determine the relevant unknown coefficients in the solutions of the relevant PDE's of heat conduction. For example, in solving the stationary, continuous point heat source problem using the PDE method, the boundary condition at the heat source is not possible to process mathematically while it is one of the simplest stationary heat source problems. Carslaw and Jaeger [2] termed problems of this type as cases of *variable temperature* and introduced an ingenious approach named the heat source method for solving such problems. It will be shown that this method can be used to solve a variety of complicated heat transfer problems in manufacturing processes and tribology with the boundary conditions where the heat fluxes are known (either a constant or a known function) but the temperatures are unknown.

The basis for the *heat source method* is the solution for the instantaneous point heat source, i.e.,

$$\theta = \frac{Q_{pt}}{c\rho(4\pi a\tau)^{3/2}} e^{-R^2/4a\tau} \tag{1}$$

Refer to the **Nomenclature** for the definition of the various parameters. Using Eq. (1) and integrating it with respect to the appropriate spatial and time variables, the solutions for an instantaneous line, plane, ring, circular disc, cylindrical surface, and spherical surface heat source as well as for continuous stationary point, line, plane, ring, and other heat sources can be obtained. A more appropriate term to describe this technique would be the *method of superposition of temperature field of individual heat sources* although for simplicity it is called the *heat source method*.

Jaeger [1] and Carslaw and Jaeger [2] presented solutions for uniform moving band and rectangular heat sources and uniform stationary heat source using the *heat source method*. In the following, a brief consideration of some representative cases of plane heat sources (both stationary and moving) in some manufacturing and tribological applications are given. For details, the readers are referred to the references cited as well as other critical reviews available in the literature.

In the manufacturing processes area, the pioneering works of Trigger and Chao [3] and Chao and Trigger [4] on the analytical evaluation of the metal cutting temperature are significant. They calculated the average tool–chip interface temperature using Jaeger's solutions for a moving band heat source (Eq. (2)), and a stationary rectangular (modified from Jaeger's solution for a stationary square) (Eqs. (2) and (3)) heat source (Eq. (3)): thus

$$\theta_M = \frac{q}{\lambda\pi}\int_{-l}^{+l} \mathrm{e}^{-v(X-X_i)/2a} K_0\left[\frac{v}{2a}\sqrt{(X-X_i)^2+z^2}\right] \mathrm{d}x_i$$

$$\theta_M = \frac{q}{\lambda\pi}\int_0^{l} \mathrm{d}x_i \int_0^{m} \frac{\mathrm{d}y_i}{\sqrt{(x-x_i)^2+(y-y_i)^2+z^2}} \tag{3}$$

They solved Eq. (3) analytically resulting in the non-dimensional temperature rise at any point at the contacting interface, θ_{xy}. The average temperature rise over the area of the chip–tool sliding contact is given by

$$\theta_{\mathrm{avg}} = \frac{1}{lm}\int_0^{l}\int_0^{m} \theta_{xy}\,\mathrm{d}x\,\mathrm{d}y$$

This equation was simplified for orthogonal (two-dimensional) cutting as: $\theta_{\mathrm{avg}} = \frac{4ql}{\pi\lambda}$*(shape factor).

Loewen and Shaw [5] (also Shaw [6]) extended Chao and Trigger's work [4] by determining the heat partition ratio for the shear plane heat source between the chip and the workmaterial as well as that for the frictional heat source between the chip and the cutting tool taking into account material properties instead of constant heat partition as used by Trigger and Chao [3]. They also developed a similar equation for the stationary rectangular heat source. However, these equations are valid only for steady state stationary heat sources of uniform heat intensity distribution, square or rectangular in shape.

In the field of tribology, Bowden and Thomas [7], Barber [8], and others (Cameron et al. [9], Gecim and Winer [10], Kuhlmann-Wildorf [11]) used similar approximate equations based on Jaeger's solution for a stationary heat source to estimate the sliding contact temperatures. Ling [12] (also, Ling and Ng [13], Ling [14]) based on the Jaeger's solution of a stationary point heat source under steady state conditions, $q_{\mathrm{pt}}/2\pi\lambda R$, used the *heat source method* to develop a solution for a stationary rectangular heat source whose intensity varies spatially: thus

$$\theta_{(x,\,y,\,z)} = \frac{1}{2\pi\lambda}\int_{-l}^{l}\int_{-b}^{b} q_1(\xi,\eta)\frac{\mathrm{d}\xi\,\mathrm{d}\eta}{R}$$

where $R = \sqrt{(x-\xi)^2+(y-\eta)^2+z^2}$. This equation offers the possibility of solving the heat source problems of various distributions of heat intensities. Francis [15] using a similar method, derived two equations for the stationary circular plane heat source — one for a uniform distribution and the other for an elliptical distribution of heat intensity.

From the late 1930's to the mid-1940's, Rosenthal [16–19], Blok [20,21], and Jaeger [1] made seminal contributions to the analysis of moving heat source problems which formed the basis for much of the applied research that followed. Because of the mathematical complexity, various moving heat source problems in manufacturing and tribology were simplified either to a moving point or a moving line heat source (Rosenthal [19]), or uniformly distributed moving band or rectangular heat source (Jaeger [13]). Also, for mathematical simplicity much of the analysis to date was limited to quasi-steady state conditions.

Rosenthal first applied the theory of heat flow due to a moving point and a moving line heat source to welding [16,17]. Based on the similarity between the differential equation of heat conduction and that in electro-magnetic waves, Rosenthal [19] considered the final solution to be a product of two separate functions — one, an exponential function $\mathrm{e}^{-vX/2a}$, which is a asymmetric function along the X-axis, and the second, $\varphi(X, y, z)$, which is a symmetric function and solved it using the moving coordinate system. The final solution is an unsymmetric function along the X-axis which is close to practice. However, for mathematical simplicity, Rosenthal considered quasi-stationary state. Mahla et al. [27] considered the method of instantaneous heat sources which is applicable to nonquasi-steady states to a particular case of welding. Rosenthal pointed out that while the solutions of Mahla et al.

does not differ significantly from that obtained on the assumption of quasi-steady state, the solutions in most cases become too unwieldy for a direct practical application.

Jaeger [1] in 1942 introduced the *heat source method* (also covered briefly in Carslaw and Jaeger [2]) for solving a wide range of moving heat source problems. He developed solutions for the temperature rise for plane heat sources of different shapes (band, square, or rectangular) starting from the solution of an instantaneous line heat source. For mathematical simplicity Jaeger considered the heating time, $t = \infty$ in the very early stages of the derivation thus limiting the analysis to quasi-steady state conditions. Jaeger not only introduced the exact solutions for uniform moving band and moving rectangular heat sources but also gave a series of approximate equations for very high and very low values of L where $L = vl/2a$ which later on became known as the Peclet number for calculating the maximum and the average temperatures over the area of the heat source. His reasons for choosing the approximate equations was to illustrate the power of the analytical techniques to address some simplified engineering problems.

Exact solutions for the moving plane heat sources problems of various shapes and heat intensity distributions were attempted only recently. Tian and Kennedy [22] using Jaeger's heat source method, developed a series of quasi-steady state solutions for moving circular, moving square, and moving elliptical heat sources of uniform and parabolic distribution of heat liberation intensity by integrating the solution of a moving point heat source with respect to appropriate spatial variables. They used polar coordinates for the circular heat source and cartesian for the rectangular heat source. Thus, their equations for the circular, square, and elliptical heat sources all seem different though mathematically correct. It also appears that the emphasis of Tian and Kennedy's work was to develop approximate solutions that would be close to the exact solutions. Bos and Moes [23], also using the heat source method, gave solutions for a moving elliptical heat source with uniform and semi-ellipsoidal distribution of heat intensity. They also developed a numerical approach to solve the steady state heat partitioning problem.

In this paper, using the *heat source method*, solutions for stationary/moving plane heat sources of various shapes (*elliptical*, *circular*, *rectangular*, and *square*) and heat intensity distributions (*uniform*, *parabolic*, and *normal*), for both *transient* and *steady state conditions* are presented. An elliptic moving heat source of various heat intensity distributions is considered as the basis and its solution is first determined. By considering the major axis of the elliptical heat source to be equivalent to the minor axis, the equation for the temperature rise for a circular heat source is obtained. Similarly, by assuming the width of the heat source to be constant, solutions for rectangular ($a_o \neq b_o$), and square ($a_o = b_o$) heat sources are obtained. Considering the velocity of the heat source, $v = 0$, the solutions for various stationary plane heat sources are obtained. It may be noted that the model developed can be applied in principle for any *geometrical* shape that can be *defined mathematically*. This analysis can similarly be extended to other distributions. Thus, the solution developed here for a single geometry (elliptical) as a basis can be extended to develop general solutions which then can be used to solve a wide range of stationary/moving plane heat source problems by merely substituting the appropriate integration limits and appropriate coefficients. Thus the analysis is considered to be comprehensive.

2. Solution for a moving point heat source

The commonly used solution of a moving point heat source [1,2]

$$\theta = \frac{q_{\mathrm{pt}}}{4\pi\lambda R} \mathrm{e}^{-(R+X)v/2a} \tag{4}$$

is applicable only for quasi-steady state conditions. Hence, to develop a general solution (for both transient and quasi-steady state) an alternate approach is needed. Fig. 1 is a schematic of the moving point heat source problem. x, y, and z form the absolute coordinate system and X, y, and z the moving coordinate system which moves along with the moving point heat source with the same velocity (along x-axis). It is required to determine the temperature rise at any point $M(x, y, z)$ and time t caused by the moving point heat source of heat intensity q_{pt} (J/s). At time τ_i, the moving point heat source had moved a distance $v\tau_i$. Thus, the distance between the heat source and the point M is given by $\sqrt{(x - v\tau_i)^2 + y^2 + z^2}$. The temperature rise, $\mathrm{d}\theta_M$ at point M at time t caused by the heat liberated in this differential infinitesimally small time interval at time τ_i (using the solution for an instantaneous point heat source Eq. (1)) is given by

$$\mathrm{d}\theta_M = \frac{q_{\mathrm{pt}}\,\mathrm{d}\tau_i}{c\rho(4\pi a\tau)^{3/2}} \exp\left[-\frac{(x - v\tau_i)^2 + y^2 + z^2}{4a\tau}\right] \tag{5}$$

The total temperature rise caused by the moving point heat source can be obtained by integrating the above equation from $\tau_i = 0$ to t, where $x - v\tau_i = x - v(t - \tau) = x - vt + v\tau$. It can be noted that $(x - vt)$ is the coordinate of the point M in the moving coordinate system in the X-direction at time t. So, it can be substituted by X. Thus, $x - v\tau_i = X + v\tau$. Set $\tau = t - \tau_i$, then

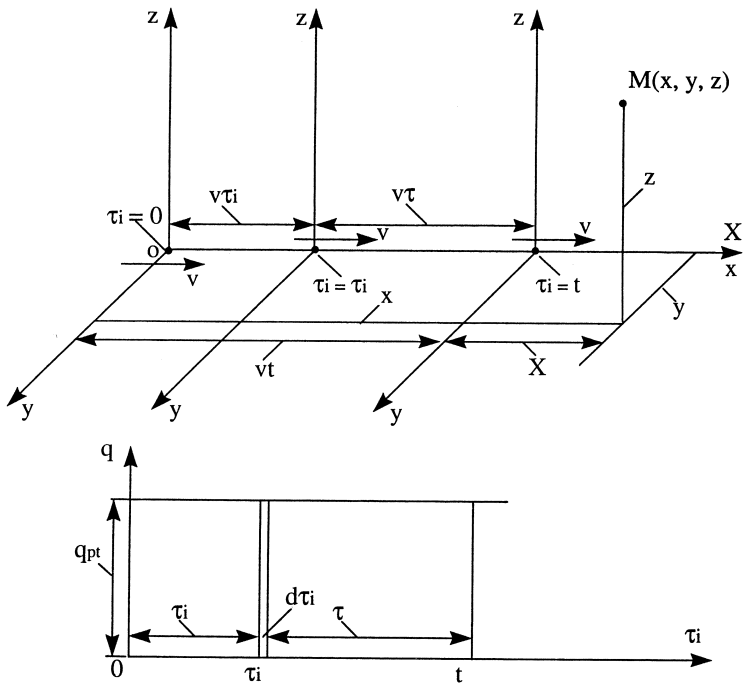

Fig. 1. Schematic showing a moving point heat source problem.

$d\tau_i = -d\tau$; when $\tau_i = 0$, $\tau = t$; when $\tau_i = t$, $\tau = 0$. It can be shown that

$$\theta_M = \frac{q_{pt}}{c\rho(4\pi a)^{3/2}} \int_{\tau=0}^{t} \frac{d\tau}{\tau^{3/2}} \exp\left[- \frac{(X + v\tau)^2 + y^2 + z^2}{4a\tau} \right] \text{or}$$

$$\theta_M = \frac{q_{pt}}{c\rho(4\pi a)^{3/2}} \exp\left(- \frac{Xv}{2a} \right) \int_{\tau=0}^{t} \frac{d\tau}{\tau^{3/2}} \exp\left[- \frac{X^2 + y^2 + z^2}{4a\tau} \right] \exp\left[- \frac{v^2\tau}{4a} \right] \tag{6}$$

To express the integral part of Eq. (6) in a non-dimensional form, it is necessary to substitute an appropriate non-dimensional term instead of variable τ. There are two possibilities: (1) $(X^2 + y^2 + z^2)/4a\tau = \xi$; and (2) $v^2\tau/4a = \omega$. Here, both ξ and ω are non-dimensional variables. Jaeger [1] used the first substitution, namely, $(X^2 + y^2 + z^2)/4a\tau = \xi$ and assumed $t = \infty$ to obtain the solution (Eq. (4)). Since this solution is time independent, it can be applied only for quasi-steady state conditions. All subsequent solutions derived based on this equation for other applications are also time independent and can be used only for quasi-steady state conditions (e.g. [22] or [23]). The use of the second substitution, namely, $v^2\tau/4a = \omega$, results in an alternate solution (Eq. (7)): thus

$$\theta_M = \frac{q_{pt} \cdot v}{16\lambda a \pi^{3/2}} \exp\left(- \frac{Xv}{2a} \right) \int_0^{\frac{v^2 t}{4a}} \frac{d\omega}{\omega^{3/2}} \exp\left[- \omega - \left(\frac{u^2}{4\omega} \right) \right] \tag{7}$$

where $u = Rv/2a$, $R = X^2 + y^2 + z^2$, R is the distance between the moving point heat source and point M where the temperature rise is of interest in the moving coordinate system at time t.

The integral part of Eq. (7) is very similar to the modified Bessel function of the second kind, order zero,

$$K_o = \frac{1}{2} \int_0^{\infty} \frac{d\omega}{\omega} \exp\left[- \omega - (u^2/4\omega) \right]$$

Eq. (7) is the solution for a moving point heat source which contains the time variable t in the upper limit of integration. The integral part of Eq. (7) is a non-dimensional coefficient. The longer the heating time t, the larger the coefficient, and higher the temperature rise at any point M. Temperature rise, therefore, is time dependent. Hence, Eq. (7) can be applied for transient conditions. This integral part has no analytical solution but can be solved numerically.

For the quasi-steady state, theoretically the heating time should be ∞ but it can be shown that for all practical purposes this value can be finite and determinable. By investigating the nature of $f(\omega)$ in Eq. (7)

for various values of u, it was found that $f(\omega)$ converges when $\omega \to 0$ and $\omega \to 5$ [24]. That is, when $\omega > 5$, no matter how large (even ∞) the results of integration are almost the same. Thus, it can be assumed that quasi-steady state condition has been established when $\omega \geq 5$, i.e. the upper limit of integration can be considered as 5, instead of ∞ for quasi-steady state. This relationship can also be used to estimate the time required for establishing the quasi-steady state conditions:

$$t_{\text{quasi-steady}} = 5\frac{4a}{v^2} = \frac{20a}{v^2}$$

As the function to be integrated also converges when $\omega \to 0$, it is necessary to consider a very small value, say 0.00001 as the lower limit of integration instead of zero. This will result in insignificant error in the final result. In this paper, Eq. (7) is used as the basis for the derivation of the general solution for moving plane heat sources of various shapes and heat intensity distributions for both transient and quasi-steady state conditions.

3. Heat liberation intensity of heat sources of various distributions

Fig. 2 is a comparison of the three heat intensity distributions, namely uniform, parabolic, and normal distributions. It shows that with the same rate of heat liberation q_{pl}, J/s, the uniform distribution has the highest uniformity, and hence the lowest maximum value of heat intensity q_0, J/cm^2·s. The normal distribution has the least uniformity and the highest maximum value of heat intensity. The parabolic distribution is in between the uniform and the normal distributions.

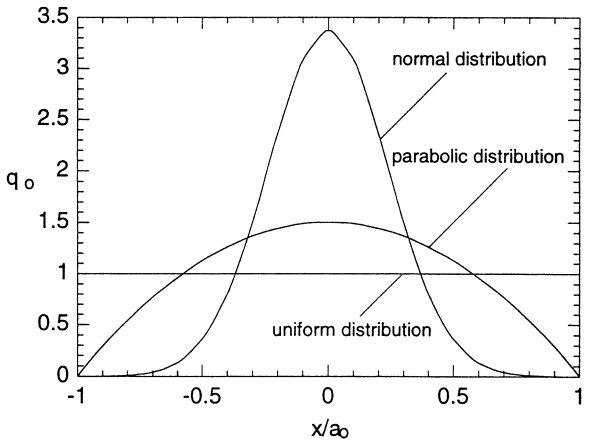

Fig. 2. Variation of the three heat intensity distributions, namely, uniform, normal, and parabolic with x_i/a_o from -1 to $+1$.

3.1. Uniform distribution

The heat intensity for various heat sources with uniform distribution is constant and given by

$$q_o = \frac{q_{\text{pl}}}{A_{\text{pl}}}$$

3.2. Parabolic distribution

Fig. 3(a) shows the variation of (2-dimensional) the heat liberation intensity of an elliptic heat source with a parabolic heat distribution. The relationship between the heat liberation intensity q_{o} and the distances x_{i} and y_{i} from the center is given by

$$q_o = C\left(1 - y_i^2/b_o^2\right)\left(1 - x_i^2/l_{y_i}^2\right)$$

The heat liberation rate from the differential area $\mathrm{d}x_i\,\mathrm{d}y_i$ is given by

$$\mathrm{d}q_{\text{ell}} = q_o\,\mathrm{d}x_i\,\mathrm{d}y_i$$

After appropriate substitutions and integration, it can be shown [25] that the heat intensity for an *elliptical heat source with a parabolic distribution* is given by

$$q_o = \frac{q_{\text{ell}}}{0.5A_{\text{ell}}}(1 - n^2)\left[1 - m^2/(1 - n^2)\right]$$

Similarly, the heat intensity for a *circular disc heat source* ($a_o = b_o$) *with a parabolic distribution* is given by

$$q_o = \frac{q_{\text{c}}}{0.5A_{\text{c}}}(1 - n^2)\left[1 - m^2/(1 - n^2)\right]$$

For a rectangular heat source with a parabolic distribution (refer to Fig. 3(b)), the relationship between the heat liberation intensity q_{o} and the distances x_{i} and y_{i} from the center is given by

$$q_o = C\left(1 - y_i^2/b_o^2\right)\left(1 - x_i^2/a_o^2\right)$$

It can be shown that the heat intensity for a *rectangular heat source with a parabolic distribution* is given by

$$q_o = \frac{q_{\text{rec}}}{4/9A_{\text{rec}}}(1 - n^2)(1 - m^2)$$

Similarly, the heat intensity for a *square heat source with a parabolic distribution* is given by

$$q_o = \frac{q_{sq}}{4/9A_{sq}}(1-n^2)(1-m^2)$$

3.3. Normal distribution

Fig. 4(a) shows the variation (2-dimensional) of the heat liberation intensity of an elliptic heat source with a normal heat distribution. The relationship between the heat liberation intensity q_o and the distances x_i and y_i from the center is given by

$$q_o = C\exp\left[-(3y_i/b_o)^2\right]\exp\left[-\left(3x_i/l_{y_i}\right)^2\right]$$

It can be shown that the heat intensity for an *elliptical heat source with normal distribution* is given by

$$q_o = \frac{q_{ell}}{0.1079A_{ell}}\exp-(3n)^2\exp\left[-\left(3m/\sqrt{1-n^2}\right)^2\right]$$

Substituting, $a_o = b_o = r_o$, the heat intensity for a *circular disc heat source with normal distribution* is given by

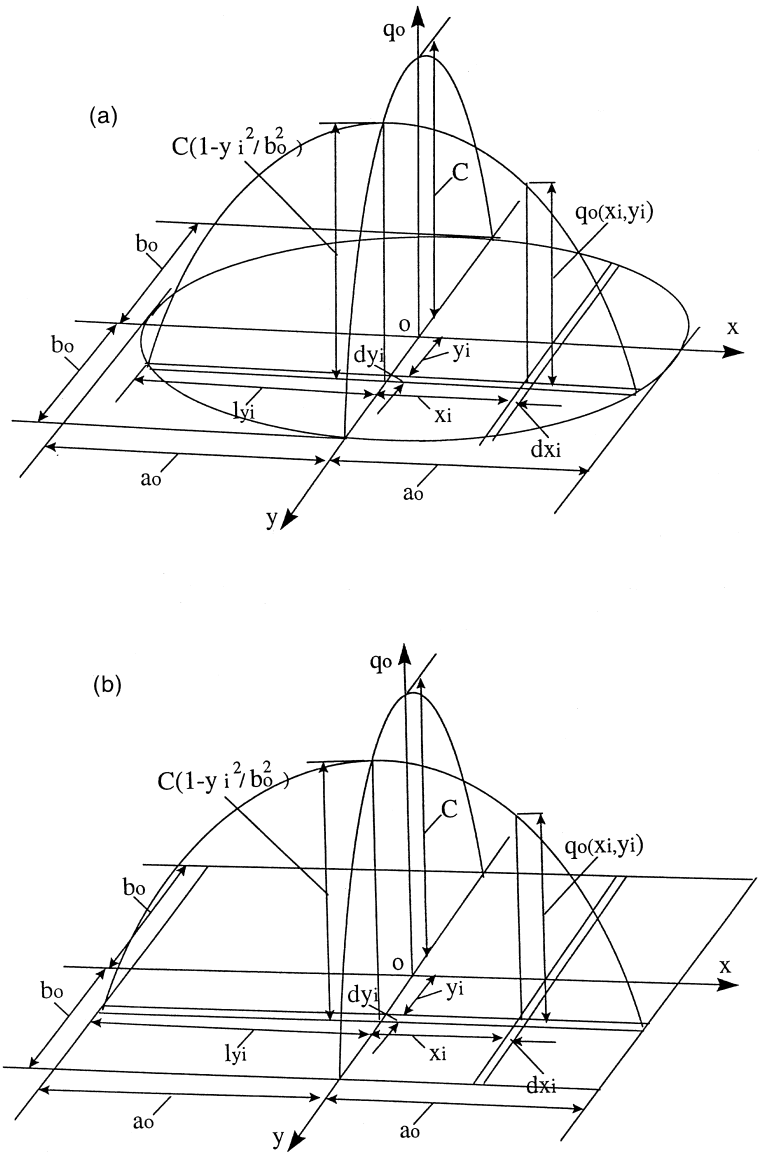

Fig. 3. (a) Variation of the heat liberation intensity of an elliptical heat source with a parabolic heat distribution. (b) Variation of the heat liberation intensity of a rectangular heat source with a parabolic heat distribution.

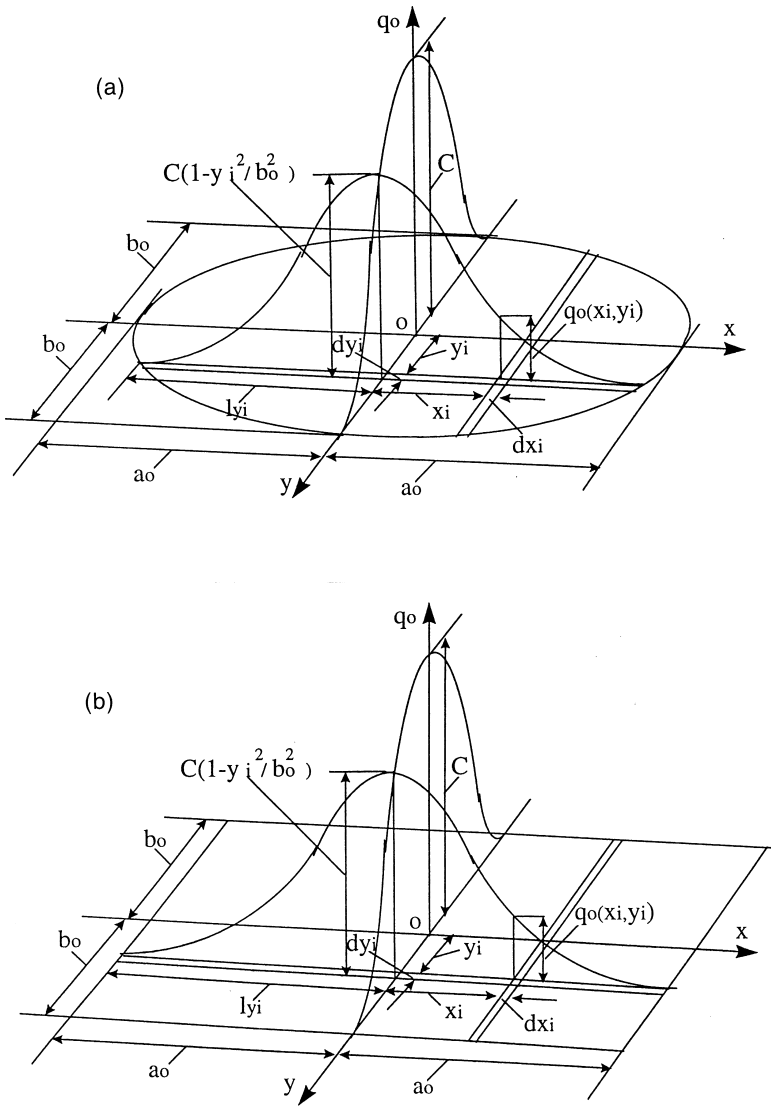

Fig. 4. (a) Variation of the heat liberation intensity of an elliptic heat source with a normal heat distribution. (b) Variation of the heat liberation intensity of a rectangular heat source with a normal heat distribution.

$$q_o = \frac{q_c}{0.1079A_c}\exp\left[-(3n)^2\right]\exp\left[-\left(3m/\sqrt{1-n^2}\right)^2\right]$$

For a rectangular heat source with a normal distribution (refer to Fig. 4(b)), the relationship between the heat liberation intensity q_o and the distances x_i and y_i from the center is given by

$$q_o = C\exp\left[-(3n)^2\right]\exp\left[-(3m)^2\right]$$

After appropriate substitutions and integration, it can be shown that the heat liberation intensity, q_o (J/cm^2·s) for a *rectangular heat source with a normal distribution* is given by

$$q_o = \frac{q_{rec}}{\pi/36A_{rec}}\exp\left[-(3n)^2\right]\exp\left[-(3m)^2\right]$$

By substituting $a_o = b_o$, we get the heat intensity for a *square heat source with a normal distribution* as

$$q_o = \frac{q_{sq}}{\pi/36A_{sq}}\exp\left[-(3n)^2\right]\exp\left[-(3m)^2\right]$$

Based on a comparison of the equations for various plane heat sources of different heat intensity distributions (Eq. (4)), a general equation for q_o can be expressed as

$$q_o = \frac{q_{pl}}{E\cdot A_{pl}}\cdot F\cdot G \tag{8}$$

Table 1
Coefficients E, F, G, and area A_{pl} for the general solution for various heat intensity distributions and various shapes of the heat sources

Shape of heat source	Distribution of intensity	E	F	G	A_{pl}
Elliptical (or circular disc)	Uniform	1	1	1	$\pi a_o b_o$
	Parabolic	0.5	$(1-n^2)$	$(1-\frac{m^2}{1-n^2})$	(or πr_o^2)
	Normal	0.1079	$\exp[-(3n)^2]$	$\exp[-(\frac{3m}{\sqrt{1-n^2}})^2]$	
Rectangular (or square)	Uniform	1	1	1	$4a_o b_o$
	Parabolic	4/9	$(1-n^2)$	$(1-m^2)$	(or $4a_o^2$)
	Normal	$\pi/36$	$\exp[-(3n)^2]$	$\exp[-(3m)^2]$	

The non-dimensional parameter E (a constant) and non-dimensional terms F and G for various heat intensity distributions are given in Table 1. For the uniform distribution E, F, and G are all equal to one.

4. General solution for moving plane heat sources

Consider the case of a moving elliptical heat source of various distributions of heat liberation intensities (Fig. 5). The rate of heat liberation of an elliptical heat source is q_{ell}, J/s. By considering the total elliptical area as a combination of stripes of different lengths of width dy_i, each stripe as a combination of numerous segments of length dX_i, and each of it as a moving point heat source, the solution of the moving point heat source, Eq. (7) can be used to calculate the temperature rise at any point M at time t caused by each of the differential segment, $dX_i dy_i$. The rate of heat liberation of this differential segment q_{pt} is given by $q_{pt} = q_o \cdot dX_i\, dy_i$, where q_o is the heat intensity of that segment of the elliptical area of the plane heat source in J/cm^2·s (refer to Figs. 3 and 5).

The area of the elliptical heat source is denoted as A_{ell}. The rate of heat liberation of this differential infinitesimal small segment $dX_i\, dy_i$ is given by

$$\frac{q_{ell}}{E \cdot A_{ell}} \cdot F \cdot G \cdot dX_i\, dy_i \quad \text{J/s}$$

The half length of the differential stripe for the elliptical heat source is a function of y_i, i.e.

$$l_{y_i} = a_o\sqrt{1-(y_i/b_o)^2} = a_o\sqrt{1-n^2} \tag{a}$$

The temperature rise, $d\theta_M$ at any point M at time t caused by each of the differential small segments $dX_i\, dy_i$ (using Eq. (7)) is given by

$$d\theta_M = \frac{q_{ell} \cdot F \cdot G \cdot dX_i\, dy_i \cdot v}{E \cdot 16\lambda a \pi^{3/2} A_{ell}} \exp\left[-\frac{(X-X_i)v}{2a}\right] \int_0^{v^2 t/4a} \frac{d\omega}{\omega^{3/2}} \exp\left(-\omega - \frac{u_i^2}{4\omega}\right) \tag{b}$$

where $u_i = R_i v/(2a)$; $R_i = \sqrt{R'^2 + z^2} = \sqrt{(X-X_i)^2 + (y-y_i)^2 + z^2}$; R_i is the distance between the differential segmental heat source $dX_i\, dy_i$ and the point M where the temperature rise is concerned.

Substituting $X_i/a_o = m$, $y_i/b_o = n$, and denoting the third integral of Eq. (6) as

$$K_m(u_i) = \int_0^{v^2 t/4a} \frac{d\omega}{\omega^{3/2}} \exp\left(-\omega - u_i^2/4\omega\right)$$

the temperature rise at any point M at time t caused by the total *elliptical moving heat source* is given by

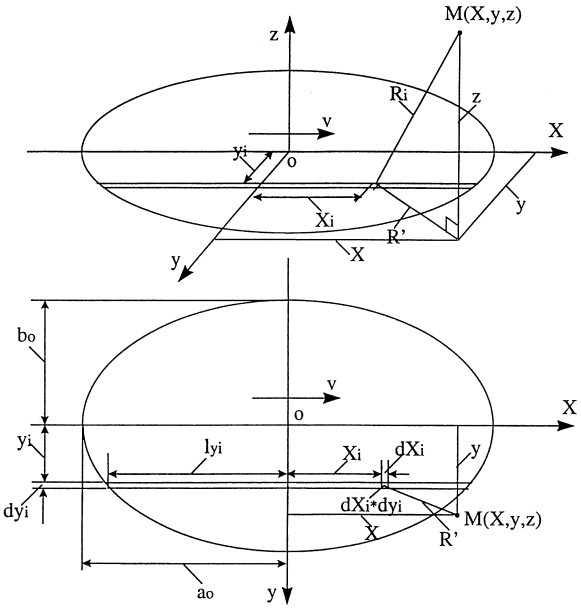

Fig. 5. Schematic showing the moving elliptic heat source problem.

$$\theta_M = \frac{q_{\mathrm{ell}} v}{E \cdot 16\lambda a \pi^{3/2} A_{\mathrm{ell}}} \int_{y_i=-b_o}^{+b_o} F \cdot \mathrm{d}y_i \int_{x_i=-a_o\sqrt{1-n^2}}^{+a_o\sqrt{1-n^2}} \mathrm{d}X_i \cdot G \cdot \exp\left[-\frac{(X-X_i)v}{2a} \right] K_m(u_i) \tag{9}$$

Eq. (9) is the general solution of a moving *elliptical heat source* of various distributions of heat intensity. A *circular disc heat source* can be considered as a special case of an elliptic heat source where $a_o = b_o = r_o$, where r_o is the radius of the circular disc. For a *rectangular heat source*, the lengths of the differential stripes are constant and equal to a_o (refer to Fig. 3(b)). A *square heat source* can be considered as a special case of a rectangular heat source, where $a_o = b_o$. It can be shown that for a moving plane heat source of various shapes, their solutions for various heat intensity distributions have the same form but differ only in the relevant limits of integration for different shapes. So, *the general solution for moving plane heat sources of various shapes and various heat intensity distributions* can be expressed as

$$\theta_M = \frac{q_{\mathrm{pl}} v}{E \cdot 16\lambda a \pi^{3/2} A_{\mathrm{pl}}} \int_{y_i=-j}^{+j} F \cdot \mathrm{d}y_i \int_{x_i=-k}^{+k} \mathrm{d}X_i \cdot G \cdot \exp\left[-\frac{(X-X_i)v}{2a} \right] K_m(u_i) \tag{10}$$

The relevant integration limits j and k for various shapes are given in Table 2.

5. The general solution for stationary plane heat sources

The stationary heat source problem can be considered as a special case of appropriate moving heat source problem when the velocity of the moving heat source v is zero (refer to Fig. 1). Consequently, $v\tau_i = 0$, $vt = 0$, thus $X = x$ and it is no longer necessary to consider the moving coordinate system. At any time τ_i the distance between the heat source and the point M (where the temperature rise is constant) is given by $\sqrt{x^2+y^2+z^2}$. The amount of heat liberated in the subsequent time interval $\mathrm{d}\tau_i$ is $q_{\mathrm{pt}}\mathrm{d}\tau_i$. This amount of heat generated can be considered as if it is liberated instantaneously, for $\mathrm{d}\tau_i$ is infinitesimally small. Thus the temperature rise at any point M near by the heat source caused by this amount of heat from the point heat source can be calculated using the solution of an instantaneous point heat source as follows:

$$\mathrm{d}\theta_M = \frac{q_{\mathrm{pt}}\,\mathrm{d}\tau_i}{c\rho(4\pi a\tau)^{3/2}} \exp\left(-\frac{x^2+y^2+z^2}{4a\tau} \right)$$

The total temperature rise at point M caused by the stationary point heat source from $\tau_i = 0$ to $\tau_i = t$ is then given by

$$\theta_M = \frac{q_{\mathrm{pt}}}{c\rho(4\pi a)^{3/2}} \int_{\tau_i=0}^{\tau_i=t} \frac{\mathrm{d}\tau_i}{\tau^{3/2}} \exp\left(-\frac{x^2+y^2+z^2}{4a\tau} \right)$$

For $\tau_i = t - \tau$, $\mathrm{d}\tau_i = -\mathrm{d}\tau$, and when $\tau_i = 0$, $\tau = t$; when $\tau_i = t$, $\tau = 0$: thus

$$\theta_M = \frac{q_{\mathrm{pt}}}{c\rho(4\pi a)^{3/2}} \int_{\tau=0}^{\tau=t} \frac{\mathrm{d}\tau}{\tau^{3/2}} \exp\left(-\frac{x^2+y^2+z^2}{4a\tau} \right) \tag{11}$$

Eq. (11) is the solution of a continuous stationary point heat source. Referring to the solution of a moving point heat source (Eq. (6)), it can be seen that when $v = 0$, the terms $\exp(-Xv/2a)$ and $\exp(-v^2\tau/4a)$ are each equal to one, and Eq. (6) becomes identically the same as Eq. (11). So, Eq. (11) is a special case of Eq. (6) when $v = 0$. The integral part of Eq. (11) cannot be solved analytically but can be calculated by numerical integration. Usually, it would be preferable to express it in non-dimensional form so that it can be used conveniently for various conditions. The integral part of Eq. (11) can be transformed into a non-dimensional form by the following substitutions. Let

$$\frac{R}{\sqrt{4a\tau}} = u \quad \text{where} \quad R = \sqrt{x^2+y^2+z^2}$$

then

$$\frac{\mathrm{d}u}{\mathrm{d}\tau} = -\frac{1}{2} R \cdot (4a\tau)^{-3/2}$$

$$4a = -2aR(4a\tau)^{-3/2}, \quad \mathrm{d}\tau = -\frac{(4a\tau)^{3/2}}{2aR}\,\mathrm{d}u;$$

$$\frac{\mathrm{d}\tau}{\tau^{3/2}} = -\frac{(4a)^{3/2}}{2aR}\,\mathrm{d}u = -\frac{4\sqrt{a}}{R}\,\mathrm{d}u$$

when $\tau = 0$, $u = \infty$; when $\tau = t$, $u = \dfrac{R}{\sqrt{4a\tau}}$.

Then, Eq. (11) can be written as

Table 2
Integration limits j and k, heat liberation rates q_{pl}, and areas for various shapes A_{pl} in the general solution

Shape	Elliptical	Circular	Rectangular	Square
j	b_o	r_o	b_o	a_o
k	$a_o\sqrt{1-(y_i/b_o)^2}$	$\sqrt{r_o^2-y_i^2}$	a_o	a_o
q_{pl} (J/s)	q_{ell}	q_{c}	q_{rec}	q_{sq}
A_{pl} (cm^2)	$\pi a_o b_o$	πr^2	$4a_o b_o$	$4a_o^2$

$$\theta = \frac{q_{pt}}{c\rho(4\pi a)^{3/2}} \frac{4\sqrt{a}}{R} \int_{u=R/\sqrt{4at}}^{u=\infty} e^{-u^2} du$$

$$= \frac{q_{pt}}{2ac\rho R\pi^{3/2}} \int_{u=R/\sqrt{4at}}^{u=\infty} e^{-u^2} du \quad (12)$$

For $\frac{2}{\sqrt{\pi}} \int_0^p e^{-u^2}\, du$, defined as an error function, $\mathrm{erf}(p) = \frac{2}{\sqrt{\pi}} \int_0^p e^{-u^2}\, du$ (see Ref. [26]).

It can be shown [27] that when $p = \infty$, $\mathrm{erf}(p) = 1$. Similarly, it can be shown [27] that

$$\int_0^{u=\infty} e^{-u^2}\, du = \frac{\sqrt{\pi}}{2}, \text{ and}$$

$$\int_0^{u=R/\sqrt{4at}} e^{-u^2}\, du = \frac{\sqrt{\pi}}{2} \mathrm{erf}\left(R/\sqrt{4at}\right)$$

Since $ac\rho = \lambda$, Eq. (12) can be written as follows, which is the solution for a stationary point heat source:

$$\theta = \frac{q_{pt}}{4\pi\lambda R}\left[1 - \mathrm{erf}\left(\frac{R}{\sqrt{4at}}\right)\right] \text{ or}$$

$$\theta = \frac{q_{pt}}{4\pi\lambda R} \cdot \mathrm{erf}\, c\left(\frac{R}{\sqrt{4at}}\right) \quad (13)$$

The general solutions for stationary plane heat sources of various shapes and heat intensity distributions can be derived starting from Eq. (13) using a method similar to the one described for the moving plane heat sources.

Substituting $q_o\, dx_i\, dy_i$ (or $\frac{q_{pl} \cdot F \cdot G}{E \cdot A_{pl}} dx_i\, dy_i$) for q_{pt} in Eq. (13), the temperature rise at any point M at any time t caused by the differential segment $dx_i\, dy_i$ (see Fig. 5) is given by

$$d\theta_M = \frac{q_{pl} \cdot F \cdot G \cdot dx_i\, dy_i}{E \cdot A_{pl} \cdot 4\pi\lambda R_i} \mathrm{erf}\, c\left(R_i/\sqrt{4at}\right).$$

Thus, the general solution for a stationary plane heat source of various shapes and heat intensity distributions is given by

$$\theta_M = \frac{q_{pl}}{E \cdot 4\pi\lambda A_{pl}} \int_{y_i=-j}^{y_i=+j} F \cdot dy_i \int_{x_i=-k}^{x_i=+k} G \frac{1}{R_i} \mathrm{erf}\, c\left(\frac{R_i}{\sqrt{4at}}\right) dx_i \quad (14)$$

where values of E, F, G, j, and k can be obtained from Tables 1 and 2.

It should be noted that Eqs. (10) and (14) are for the case of an infinite conduction medium. In most practical cases when the conduction medium is a *semi-infinite body* and the heat source is moving or remaining stationary on its boundary surface, the results of calculation using Eqs (10) and (14) should be doubled for a *semi-infinite body*. Thus, the general solution for a moving plane heat source in a semi-infinite body is given by

$$\theta_M = \frac{q_{pl} v}{E \cdot 8\lambda a\pi^{3/2} A_{pl}} \int_{y_i=-j}^{+j} F \cdot dy_i \int_{x_i=-k}^{+k} dX_i \cdot G \cdot \exp\left[-\frac{(X - X_i)v}{2a}\right] K_m(u_i) \quad (15)$$

The general solution of a *stationary plane heat source* in a *semi-infinite body* is given by

$$\theta_M = \frac{q_{pl}}{E \cdot 2\pi\lambda A_{pl}} \int_{y_i=-j}^{y_i=+j} F \cdot dy_i \int_{x_i=-k}^{x_i=+k} G \frac{1}{R_i} \mathrm{erf}\, c\left(\frac{R_i}{\sqrt{4at}}\right) dx_i \quad (16)$$

6. Results and discussion

6.1. Surface temperature rise distribution, flash temperatures, and flash durations due to a moving plane heat source

There are different critical temperatures and corresponding flash durations that should be considered in the optimization of various advanced manufacturing processing technologies, such as the critical temperatures for certain in situ chemical reactions to take place as in chemo-mechanical polishing of advanced ceramics, or for the diffusion of certain species for improving corrosion resistance, or for certain phase transformation to take place for improving the hardness or toughness, etc. The flash temperatures and relevant flash durations can be predicted using the surface temperature rise distribution plots which in turn are calculated using the general solution for moving plane heat sources in a semi-infinite medium, Eq. (15).

Fig. 6(a)–(f) show the variation of the non-dimensional temperature rise $T(= \theta_M \lambda a/q_{pl} v)$ distributions on the surface of a semi-infinite conduction body along the direction of motion, X, and through the center of the heat source ($y = 0$) for an *elliptic heat source* of various heat intensity distributions and different Peclet numbers, $N_{Pe}[N_{Pe} = va_o/2a$, where v is the moving velocity of the heat source, m/s, a_o is the semi-length of the heat source along the direction of motion, cm, and a is the thermal diffusivity, $cm^2/s]$. Similar distributions can be obtained for heat sources of different shapes, such as circular, rectangular, and square. Peclet number, N_{Pe} is a convenient non-dimensional expression

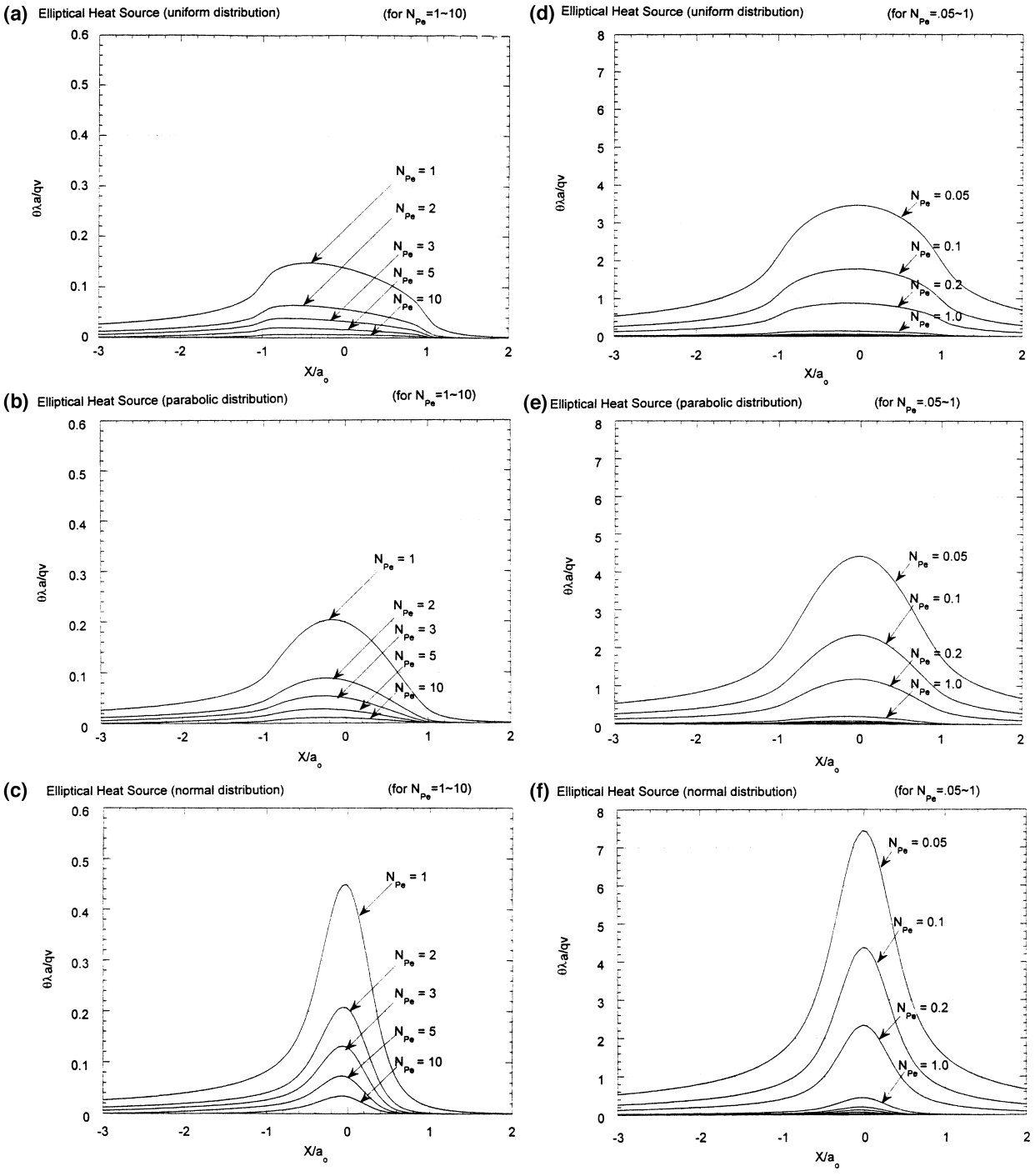

Fig. 6. (a)–(f) Variation of the non-dimensional temperature rise distribution ($\theta\lambda a/qv$) along the direction of motion (X) and through the center ($y = 0$) of an *elliptic heat source* with uniform, parabolic, and normal distributions of heat intensity, respectively, with X/a_o for Peclet numbers of 1–10 and 0.05–1.

for the relative velocity of motion of the heat source considering the thermal properties of the conduction medium which determines the speed of dissipation of heat in the medium. Peclet numbers in the range of 0–10 are generally encountered in most manufacturing and tribological problems. However, since in this range the values of T (non-dimensional temperature rise) can vary significantly, two sets of plots are made here for clarity, i.e., $N_{Pe} = 0.05$–1, and $N_{Pe} = 1$–10. It can be seen that the symmetry of the non-dimensional temperature rise distribution increases with decrease in the Peclet number. Also, the maximum temperature rise is near the rear edge when the Peclet number is large and moves towards the center with decrease in the Peclet number. Also, the maximum temperature rise is closer to the center of the heat source towards the rear edge for the normal distribution and moves further away towards the rear edge for the parabolic, followed by the uniform distribution. The similarity in the nature of the curves for a given heat distribution (uniform, parabolic, and normal) can be clearly seen. It can be seen from Fig. 6, the location of maximum temperature rise is different for different Peclet numbers and different heat intensity distributions. When N_{Pe} is very

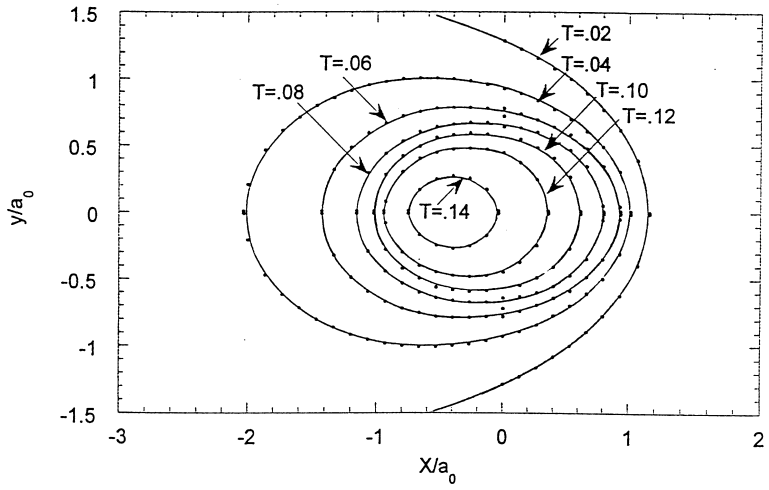

(a) Uniform distribution

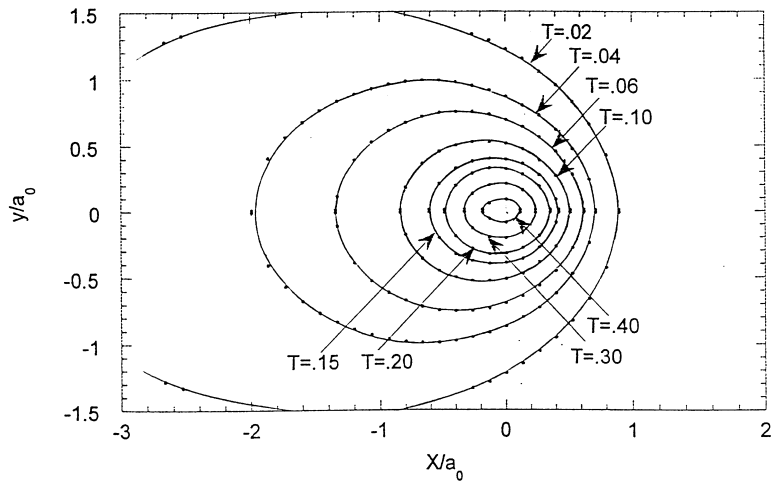

(b) Normal distribution

Fig. 7. (a)–(b) Non-dimensional temperature rise isotherms on the surface for an elliptical heat source with uniform and normal heat intensity distributions, respectively for $N_{\mathrm{pe}} = 1$. The non-dimensional temperature rise, $T = \theta\lambda a/qv$.

large (say $N_{Pe} = 10$), for a uniform distribution, the location of the maximum temperature rise is $\sim 0.78(X/a_o)$ towards the trailing edge of the moving heat source. For parabolic distribution, it is $\sim 0.3(X/a_o)$ and for the normal distribution it is ~ 0.1, or, very near the center of the moving heat source.

Fig. 7(a) and (b) show the non-dimensional temperature rise, T $(= \theta_M \lambda a/q_{\mathrm{pl}} v)$ isotherms on the surface for an *elliptical* heat source with *uniform* and *normal* distributions for $N_{Pe} = 1$. It can be seen that the peak temperature rise for the case of normal distribution is near the center of the heat source while that for a uniform distribution is between the center and the rear edge of the heat source. Together with Fig. 6, they show the temperature distributions on the surface based on the results of the temperature rise calculations using the general solution of the moving plane heat sources for a semi-infinite medium (Eq. (15)). Such information is extremely valuable for the determination of the expected flash temperatures and corresponding flash durations.

Rosenthal [2] used moving point and moving line heat source models in determining the temperature distribution in welding. Actually the heat source in welding is a moving plane heat source. To approximate it to a point or a line source, the temperature rise calculated for those points near the heat source will always be higher than actual. The closer the point to the source, the larger the error. Of course, for the point at the center of the heat source it would be infinity. Rosenthal plotted the temperature distribution contours using his analysis and compared it experimentally. He pointed out that only the points beyond a distance of 6–8 mm from the heat source gave satisfactory agreement with the experimental results and cautioned regarding the accuracy of values closer to the heat source. Consequently, such an approximation leads to a loss of significant information at and near the heat source. The general solutions for various moving plane heat sources developed in this investigation enable calculations of the temperatures very close to the plane heat source or even at the center of it with sufficiently high accuracy.

6.2. Surface temperature rise distribution due to stationary plane heat sources

Fig. 8 shows isotherms of the temperature rise distribution on the surface of a body due to an *elliptical stationary heat source with a normal, parabolic, and uniform distribution of heat intensity*, respectively. It can be seen that for the uniform distribution, the change of temperature rise from the periphery to the center of the heat source ($x/a_0 = \pm 1$ to 0) is not large and varies from ~ 0.7 to 1.17. For the normal distribution, it varies from ~ 0.5 to 2.97 accompanied by a high temperature peak of ~ 1.8 to 2.97 in the near central region ($x/a_0 = -0.3$ to $+0.3$). For the parabolic distribution, the value is somewhere in between. This means the distribution of temperature rise for a uniform elliptical heat source is comparatively flat while that for the normal elliptical heat source it is rather steep near the center region. For the parabolic elliptical heat source it is somewhere in between.

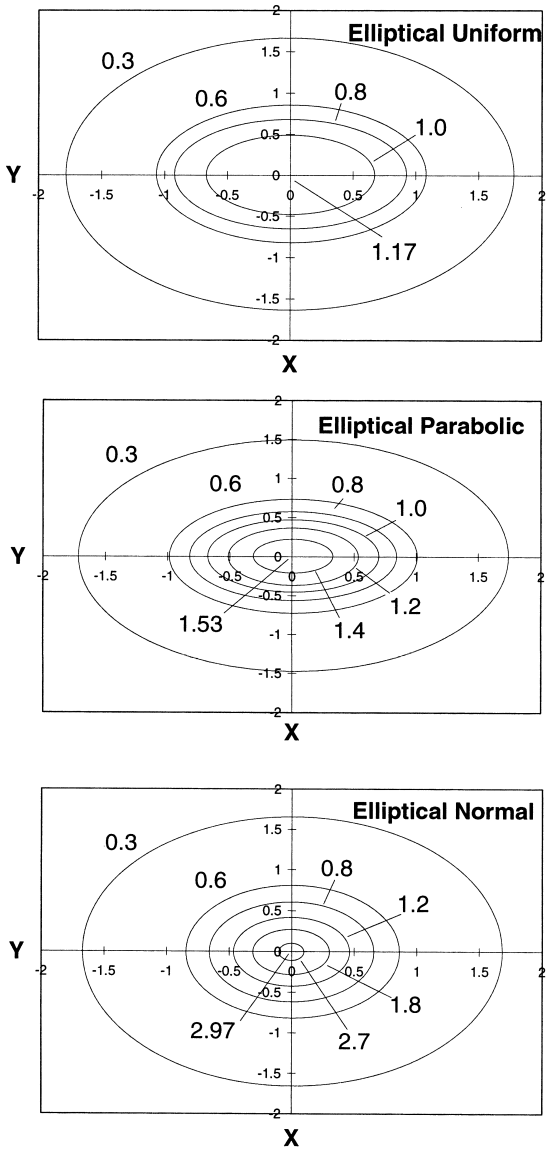

Fig. 8. (a)–(c) Isotherms of the non-dimensional temperature rise distribution on the surface of a body due to an elliptical heat source with (a) uniform, (b) parabolic, and (c) normal distributions of heat intensity, respectively.

6.3. On the estimation of the time required for establishing the steady state conditions for stationary plane heat sources

Fig. 9(a)–(c) show the variation of the non-dimensional temperature rise distribution on the surface using the general equation for a semi-infinite medium (Eq. (16)) for a *stationary elliptical heat source* of various heat intensity distributions, namely, *uniform*, *parabolic*, and *normal*, respectively. Each figure contains a set of temperature distribution curves for different heating times ($t = 1$, 10 and 100 μs, 1 and 10 ms as well as for the steady state). It can be seen from Fig. 9(a), that when $t \geq 10$ ms, the temperature rise caused by the stationary heat sources is very close to the values for the steady state. From a practical consideration, it is, therefore, not necessary to consider $t = \infty$ for reaching the steady state conditions but a finite value instead. However, this involves the acceptance of a small error. Depending on the allowable error, the time required for establishing the steady state may not be very long. Practically, when the radius of the area of concern is ~ 1–2.5 times that of the heat source and the allowable error is about 1%, the time required for reaching the steady state is usually finite and on the order of ~ 0.1–1 s.

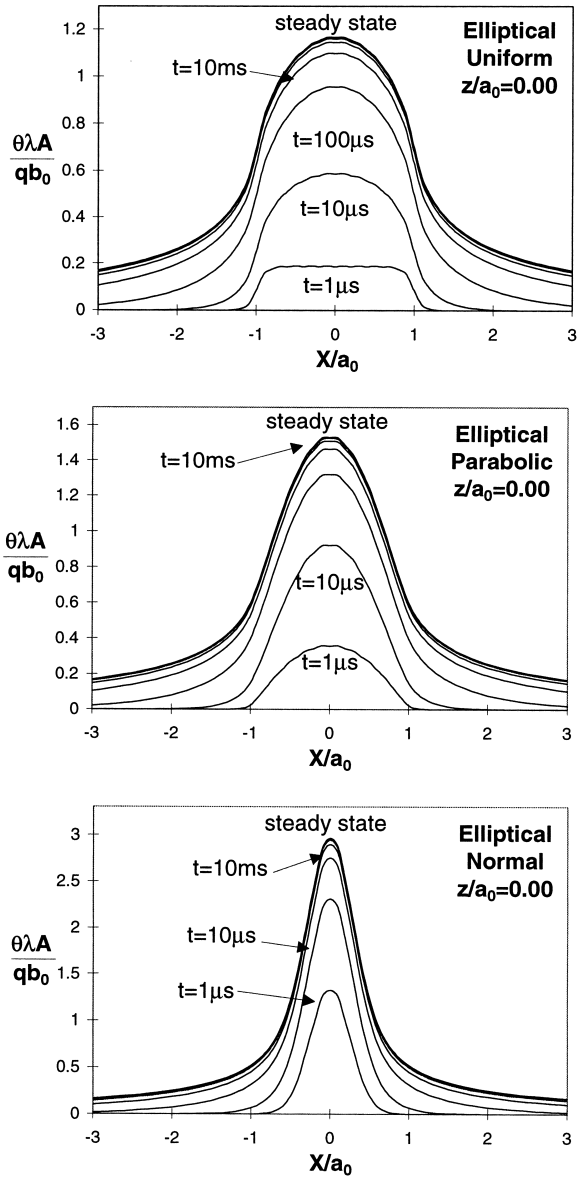

Fig. 9. (a)–(c) Variation of the non-dimensional temperature rise on the surface with x_i/a_o from -3 to $+3$ due to an elliptical heat source with (a) uniform, (b) parabolic, and (c) normal distributions of heat intensity, respectively.

6.4. Temperature distribution under the surface

Temperature distribution under the surface is very important in many manufacturing applications. For example, surface integrity including metallurgical changes at and near the surface, and the residual stresses are affected by the temperature gradients from the surface into the interior. Hence, it is desirable to know not only the temperature at the surface but also the distribution of the temperature under the surface. Fig. 10(a) and (b) show the variation of the non-dimensional temperature distribution under the surface of a body along the X-axis in the X–o–z plane of the moving coordinate system due to an elliptical moving heat source of *uniform* and *normal* distributions, respectively for different Peclet numbers (1, 5, and 10), where the origin of the moving coordinate system coincides with the center of the heat source. X/a_o and z/a_o are non-dimensional distances from the center of the heat source and the depth, respectively. Fig. 10(a) and (b) show that the temperature gradient is rather steep initially followed by a gradual change with increasing depth. Also, the temperature gradient is much steeper at higher values of Peclet numbers.

Based on the variation of the temperature rise in the heat conduction body under the point where the maximum temperature rise takes place with depth, the following approximate equations for the calculation of the non-dimensional temperature distribution under the surface at the point of maximum surface temperature at different depths are obtained.

$\theta = 0.14578 N_{Pe}^{-1.15} \mathrm{e}^{-(0.56742+0.6796 N_{Pe})z/a_o}$ (for an elliptical *uniform* heat source)

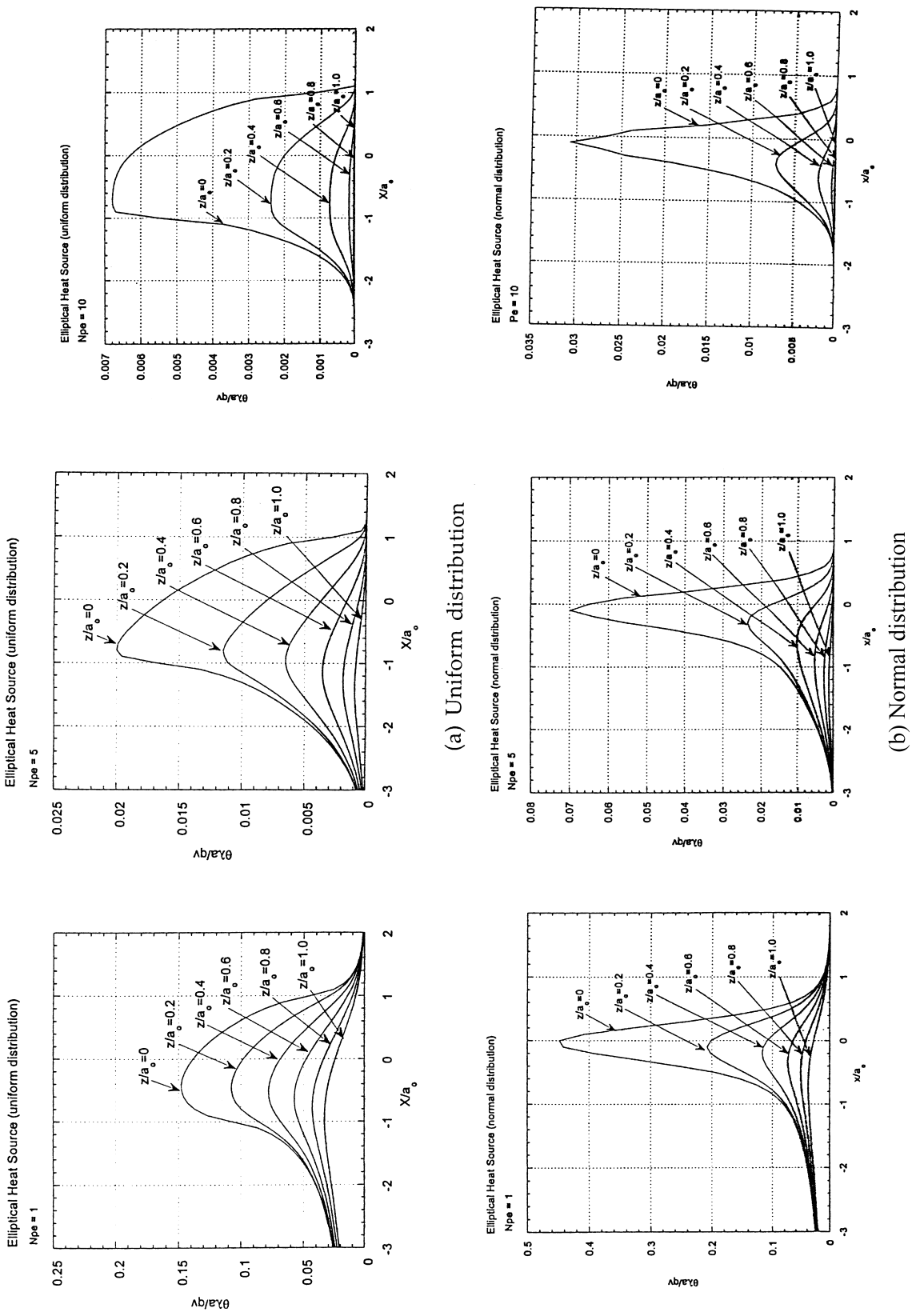

Fig. 10. (a)–(b) Variation of the non-dimensional temperature rise under the surface, along the X-axis, in the X–o–z plane of the moving coordinate system X–y–z (where the origin coincides with the center of the heat source for an elliptical heat source) of uniform and normal distributions, respectively, for different Peclet numbers (1, 5, and 10).

$$\theta = 0.36271 N_{Pe}^{-0.98862} e^{-(1.8388+0.82371 N_{Pe})z/a_o}$$

(for an elliptical *normal* heat source)

Fig. 11(a) and (b) show the variation of the temperature rise under the maximum surface temperature point on the surface with depth for an elliptical heat source with uniform and normal heat distributions, respectively, for values of Peclet numbers in the range of 0.1–10. Here, the logarithmic scale is adopted for the non-dimensional temperature rise axis as these values are distributed over a very wide range (from 6×10^{-6} to 5). They show that higher the Peclet number, the steeper the temperature gradient which is an important factor in determining the residual stresses and subsurface damage in such manufacturing processes as grinding. It can also be seen that the gradient of the temperature drop from the surface to a given depth, say $z/a_o = 0.2$ or 0.3, for a normal elliptical heat source is higher than for a uniform elliptical heat source.

Using the general solution for the stationary plane

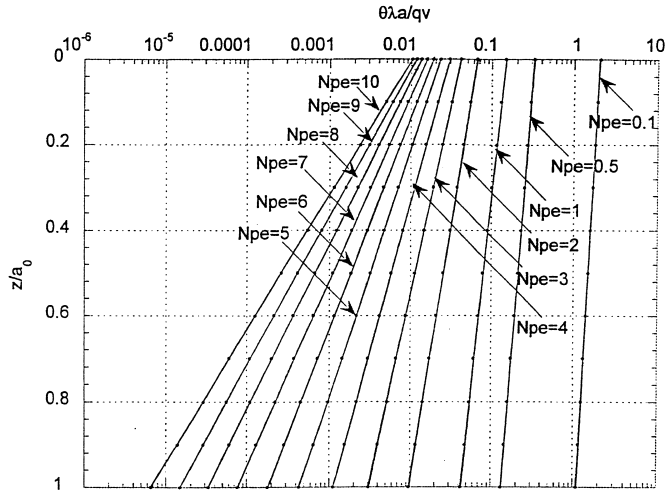

(a) Uniform distribution

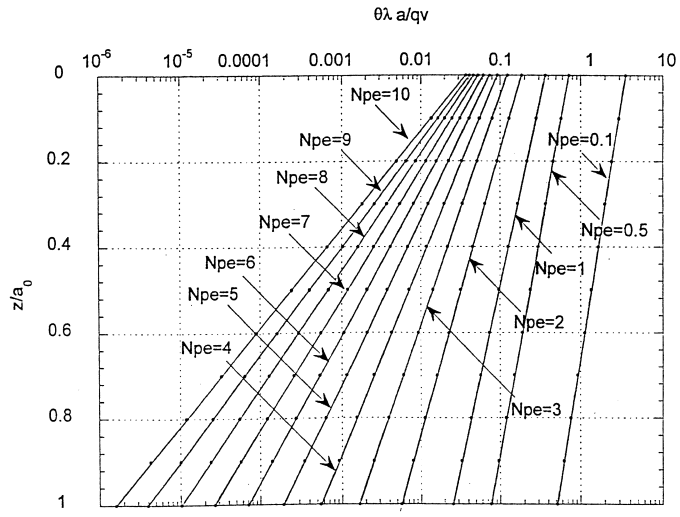

(b) Normal distribution

Fig. 11. (a)–(b) Variation of the non-dimensional temperature rise distribution ($\theta\lambda a/qv$) under the maximum temperature point on the surface with z/a_o for an elliptic heat source for various Peclet numbers with uniform and normal distributions, respectively, using the approximate equations.

heat sources for a semi-infinite medium (Eq. (16)), the temperature rise distributions under the surface caused by the stationary plane heat source can be calculated. Fig. 12 shows the distribution of the steady state temperature rise at different depths under the surface of the body and Fig. 13 shows the steady state distribution of the temperature rise along the z-axis under the point of maximum surface temperature. It can be seen from Fig. 13 that for the cases of stationary heat sources the temperature gradient is low for a uniform heat source, much higher for a parabolic heat source, and even higher for the normal heat source.

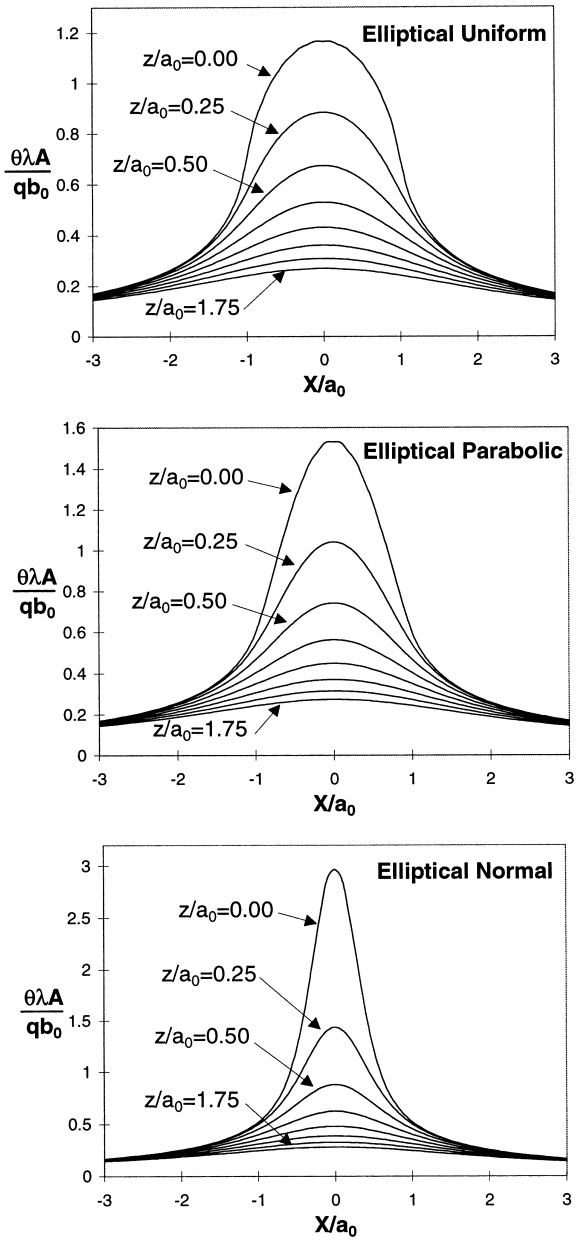

Fig. 12. (a)–(c) Variation of the non-dimensional temperature rise at different depths under the surface of a body with x_i/a_o from -3 to $+3$ due to an elliptical heat source of (a) uniform, (b) parabolic, and (c) normal distributions of heat intensity.

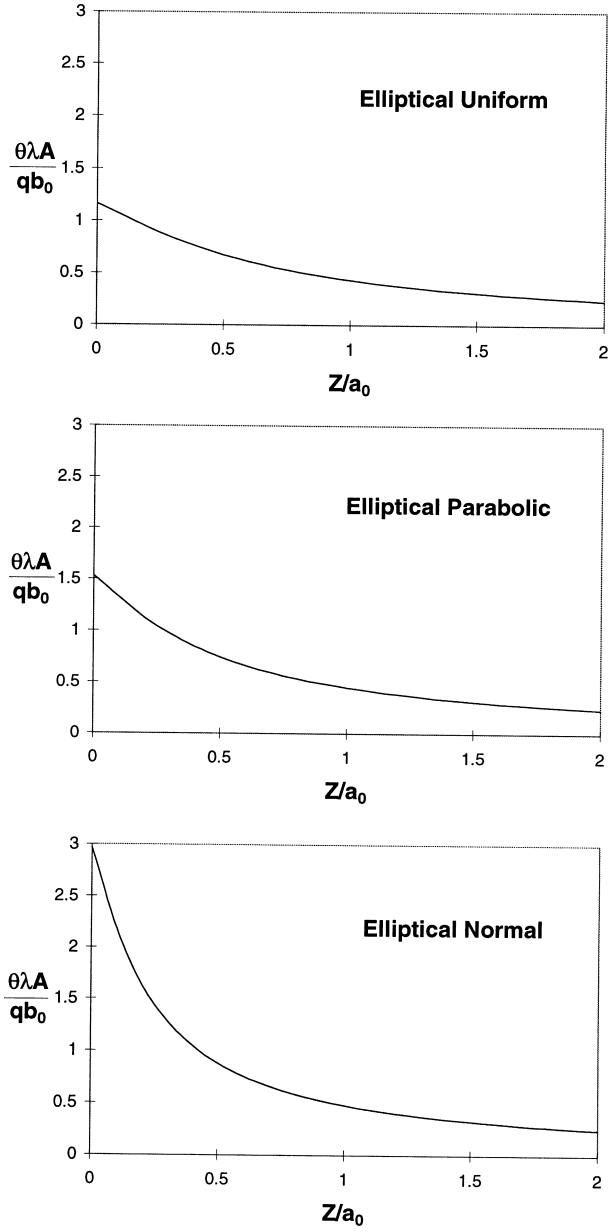

Fig. 13. (a)–(c) Variation of the maximum non-dimensional temperature rise under the surface of a body with z/a_o from 0 to $+2$ due to an elliptical heat source of (a) uniform, (b) parabolic, and (c) normal distributions of heat intensity, respectively.

7. Conclusions

1. The *general solutions* for the temperature rise at any point (Eq. (15)) for various moving heat sources and (Eq. (16)) for various stationary heat sources caused by various stationary and moving plane heat sources of different shapes (*elliptical*, *circular*, *rectangular*, and *square*) and heat intensity distributions (*uniform*, *parabolic*, and *normal*) were developed based on Jaeger's classical *heat source method*. These equations can be used for both *transient* and *steady state* conditions. They can also be used for determining the *temperature distribution on the surface* as well as *with respect to the depth*. Only one program is sufficient for computation which is very convenient for addressing a range of manufacturing and tribological problems.
2. The *general solution* for moving plane heat sources can be used for transient conditions when $v^2t/4a < 5$ and for quasi-steady state conditions when $v^2t/4a = 5$. This relationship can also be used to estimate the time required for establishing the quasi-steady state conditions, namely, $t_{\text{quasi-steady}} = 5[4a/v^2]$.
3. Using the general solution for the temperature rise at any point due to various moving heat sources, the temperature rise (non-dimensional or dimensional) isotherms on the surface can be plotted. This information is valuable for the determination of the flash temperatures and the corresponding flash durations which play an important role in the optimization of various advanced manufacturing technologies for improving the quality, productivity, and cost.
4. For moving heat sources, the location of the point of maximum temperature rise is shown to be different for different Peclet numbers and heat intensity distributions. When N_{Pe} is very large (say $N_{Pe} = 10$), for a uniform distribution, it is $\sim 0.78(X/a_o)$ towards the trailing edge of the moving heat source. For parabolic distribution, it is $\sim 0.3(X/a_o)$ and for the normal distribution it is about 0.1 or very near the center of the moving heat source.
5. For moving heat source problems, the magnitude of the temperature rise as well as its distribution around the heat source depends on several factors, including the heat intensity and its distribution, the shape and size of the heat source, the thermal properties, and the velocity of sliding (usually the non-dimensional Peclet number is used to express the relative sliding velocity considering the thermal properties and the size of heat source). It was shown that the symmetry of the non-dimensional temperature rise distribution increases with decrease in the Peclet number.
6. Temperature rise distribution under the surface can also be calculated using the general solution developed in this investigation. Temperature gradients from the surface into the interior play a very important role in many manufacturing applications and affect the surface integrity including metallurgical changes at and near the surface and the residual stresses. The results obtained show that the temperature gradient is steep initially followed by a gradual change with increasing depth. The temperature gradient is much steeper at higher values of the Peclet numbers. It is also different for different heat intensity distributions — steeper for normal, less steeper for parabolic, and even less steeper for uniform distribution.

Acknowledgements

This project is sponsored by grants from the National Science Foundation on "Tribological Interactions in Polishing of Advanced Ceramics and Glasses," (CMS-94-14610) and "Design, Construction, and Optimization of Magnetic Field Assisted Polishing," (DMI-94-02895), and DoD's DEPSCoR Program on "Finishing of Advanced Ceramics," (DAAH 04-96-1-0323). This project was initiated by an ARPA contract on "Ceramic Bearing Technology Program," (F33615-92-5933) and an NSF U.S.–China cooperative research project on the Thermal Aspects of Manufacturing. Thanks are due to Drs. J. Larsen Basse, B.M. Kramer, Ming Leu, Delci Durhan, and A. Hogan of NSF and Dr. K.R. Mecklenburg of WPAFB and Dr. W. Coblenz of DARPA for their interest in and support of this work.

References

[1] J.C. Jaeger, Moving sources of heat and the temperature at sliding contacts, Proc. Roy. Soc. NSW 76 (1942) 203–224.
[2] H.S. Carslaw, J.C. Jaeger, Conduction of Heat in Solids, 2nd ed., Oxford University Press, Oxford, 1959.
[3] K.J. Trigger, B.T. Chao, An analytical evaluation of metal-cutting temperatures, Trans. ASME 73 (1951) 55–68.
[4] B.T. Chao, K.J. Trigger, Cutting temperatures and metal cutting phenomena, Trans. ASME 73 (1951) 777–787.
[5] E.G. Loewen, M.C. Shaw, On the analysis of cutting tool temperatures, Trans. ASME 76 (1954) 217–231.
[6] M.C. Shaw, Metal Cutting Principles, Oxford University Press, Oxford, 1984.

[7] F.P. Bowden, P.H. Thomas, Surface temperatures of sliding solids, Proc. Roy. Soc. A 223 (1953) 29–39.
[8] J.R. Barber, Distribution of heat between sliding surfaces, J. Mech. Eng. Sci 9 (1967) 351–354.
[9] A. Cameron, A.N. Gordon, G.T. Symm, Contact temperatures in rolling/sliding surfaces, Proc. Roy. Soc. (1964) 45–61.
[10] B. Gecim, W.O. Winer, Transient temperatures in the vicinity of an asperity contact, Trans. ASME, J. Tribology 107 (1985) 333–342.
[11] D. Kuhlmann-Wildorf, Flash temperatures due to friction and Joule heat at asperity contacts, Wear 105 (1985) 187–198.
[12] F.F. Ling, A quasi-Iterative method for computing interface temperature distributions, Zeitschrift fur Angewandte Mathematik X (1959) 461–474.
[13] F.F. Ling, C.W. Ng, On temperatures at the interfaces of bodies in sliding contact, in: Proc. of Fourth U.S. Nat. Congr. of Appl. Mech., ASME, New York, vol. 4, 1962, pp. 1343–1349.
[14] F.F. Ling, Surface Mechanics, Wiley/Interscience, New York, 1973.
[15] H.A. Francis, Interfacial temperature distribution within a sliding hertzian contact, ASLE Trans. 14 (1970) 41–54.
[16] D. Rosenthal, Theoretical study of the heat cycle during arc welding (in French), in: 2-eme Congres National des Sciences, Brussels, 1935, pp. 1277–1292.
[17] D. Rosenthal, Mathematical theory of heat distribution during welding and cutting, Welding Researach Supplement (1941) 220s–234s.
[18] D. Rosenthal, R. Schmerber, Thermal study of arc welding — experimental verification of theoretical formulas, Welding Research Supplement (1938) 2–8.
[19] D. Rosenthal, The theory of moving sources of heat and its application to metal treatments, Trans. ASME 80 (1946) 849–866.
[20] H. Blok, Theoretical study of temperature rise at surfaces of actual contact under oiliness lubricating conditions, in: Proc. of the General Discussion on Lubrication and Lubricants, vol. 2, Inst. of Mech. Engrs., London, 1937, pp. 222–235.
[21] H. Blok, The dissipation of frictional heat, Appl. Sci. Res., Section A 5 (1955) 151–181.
[22] X. Tian, F.E. Kennedy Jr, Maximum and average flash temperatures in sliding contact, Trans. ASME, J. Tribology 116 (1994) 167–174.
[23] J. Bos, H. Moes, Frictional heating of tribological contacts, Trans. ASME, J. Tribology 117 (1995) 171–217.
[24] Z.B. Hou, R. Komanduri, Magnetic field assisted finishing of ceramics, Part I: thermal model, Trans. ASME, J. Tribology 120 (1998) 645–651.
[25] Z.B. Hou, R. Komanduri, General solutions for plane heat source problems in manufacturing and tribology, Part I: stationary heat sources, Part II: moving heat sources, MAE Research Report, Oklahoma State University, Stillwater, OK, 1998.
[26] M.R. Spiegel, Mathematical Handbook of Formulas and Tables, Schaum's Outline Series, McGraw-Hill, New York, 1993.
[27] E.M. Mahla, M.C. Rowland, C.A. Shook, G.E. Doan, Heat flow in arc welding, Welding Journal 20 (1941) 459.